Influence of Si doping on the structural and optical properties of InGaN epilayers*

Lu Ping-Yuan(卢平元)[a)b)], Ma Zi-Guang(马紫光)[b)], Su Shi-Chen(宿世臣)[a)], Zhang Li(张 力)[a)], Chen Hong(陈 弘)[b)†], Jia Hai-Qiang(贾海强)[b)], Jiang Yang(江 洋)[b)], Qian Wei-Ning(钱卫宁)[a)], Wang Geng(王 耿)[a)], Lu Tai-Ping(卢太平)[b)], and He Miao(何 苗)[a)‡]

[a)] *Laboratory of Nanophotonic Functional Materials and Devices, Institute of Optoelectronic Materials and Technology, South China Normal University, Guangzhou* 510631, *China*

[b)] *Beijing National Laboratory of Condensed Matter, Institute of Physics, Chinese Academy of Sciences, Beijing* 100080, *China*

(Received 8 January 2013; revised manuscript received 11 April 2013)

Influences of the Si doping on the structural and optical properties of the InGaN epilayers are investigated in detail by means of high-resolution X-ray diffraction (HRXRD), photolumimescence (PL), scanning electron microscope (SEM), and atomic force microscopy (AFM). It is found that the Si doping may improve the surface morphology and crystal quality of the InGaN film and meanwhile it can also enhance the emission efficiency by increasing the electron concentration in the InGaN and suppressing the formation of V-defects, which act as nonradiative recombination centers in the InGaN, and it is proposed that the former plays a more important role in enhancing the emission efficiency in the InGaN.

Keywords: Si doping, InGaN, V-shaped defect

PACS: 68.55.Jk, 68.55.Ln, 78.60.Hk, 78.66.Fd **DOI:** 10.1088/1674-1056/22/10/106803

1. Introduction

In recent years, structural and optical properties of InGaN have aroused great interest because of its widespread applications in light-emitting devices such as light-emitting diodes (LEDs) and laser diodes.[1–6] Meanwhile, high emission efficient InGaN is proposed as a potential novel fluorescent material for field emission display (FED), which is possible to work at a low acceleration voltage (42 V) compared with the traditional phosphor.[7] It has also been reported that InGaN material was introduced into a single chip white light emitting diode as an underlying layer (UL) embedded below an active layer of InGaN/GaN multiple quantum wells, and the quality of the white light could be controlled by modulating the relaxation degree of the InGaN UL.[8] However, structural defects, e.g. threading dislocations, pits or V-shaped defects in InGaN layers have seriously restricted the progress of InGaN-based devices. Therefore, improving the quality of InGaN is vital to accelerate the development of InGaN-based devices. Also, it has been reported that Si doping in GaN barriers improves the interface quality and optical property of InGaN/GaN multiple quantum wells.[9–11] However, the influence of Si doping in InGaN film on the structural and optical properties still needs further study. In this work, InGaN films with different Si concentrations are deposited by low-pressure metal–organic vapor epitaxy (LP-MOVPE). High-resolution X-ray diffraction (HRXRD), photoluminescence (PL), scanning electron microscope (SEM), and atomic force microscopy (AFM) are employed to characterize the structural and optical properties of InGaN.

2. Experiment

All the samples were grown on *c*-plane sapphire substrates in an LP-MOVPE system. The common two-flow method was used in the growth of GaN film in which a 30-nm thick GaN buffer layer was grown at 500 °C followed by 3-μm-thick GaN films at high temperature about 1050 °C.[12] Then the InGaN films were deposited on GaN buffer layers at a temperature of about 800 °C and a pressure of 26 kPa in order to achieve low indium content. The experimental conditions in our work were optimized in our MOVPE system to obtain good crystal quality epilayers. Trimethylgallium (TMGa), trimethylindium (TMIn), and ammonia (NH_3) were used as the precursors. Silane (SiH_4) was used as the n-type dopant. InGaN films with thickness varying from 100 nm to 500 nm were deposited in order to study the influence of film thickness on the properties of the InGaN. The 500-nm thick InGaN films with different doping concentrations were deposited and the growth parameters were the same except for the mole flow

*Project supported by the National High Technology Research and Development Program of China (Grant Nos. 2011AA03A112, 2011AA03A106, and 2013AA03A101), the National Natural Science Foundation of China (Grant Nos. 11204360, 61210014, and 61078046), the Science & Technology Innovation Program of Department of Education of Guangdong Province, China (Grant No. 2012CXZD0017), the Industry–Academia Research Union Special Fund of Guangdong Province, China (Grant No. 2012B091000169), and the Science & Technology Innovation Platform of Industry–Academia Research Union of Guangdong Province–Ministry Cooperation Special Fund, China (Grant No. 2012B090600038).

†Corresponding author. E-mail: hchen@aphy.iphy.ac.cn

‡Corresponding author. E-mail: herofate@126.com

© 2013 Chinese Physical Society and IOP Publishing Ltd

rate of SiH_4 (0, 0.32, 1.28, 2.24, and 3.2 nmol/min). The doping concentrations were obtained from the Hall measurements. The HRXRD was employed to characterize the quality of the InGaN films. The PL spectra were recorded using a 325-nm He–Cd continuous wave laser at an emission power of about 20 mW. The emitted light was dispersed by a triple grating monochromator and detected by the GaAs photomultiplier tube using a conventional lock-in technique. The surface morphologies of the samples were characterized by SEM and AFM.

3. Result and discussion

First, we study the influence of film thickness on the properties of the InGaN film. The results show that the increase of film thickness leads to the decline in crystal quality of the InGaN and meanwhile the relaxation degree of the InGaN film increases and more indium atoms are incorporated into the film with the increase of the film thickness. Figures 1(a) and 1(b) display the reciprocal space mapping (RSM) around the (1 0 5) reflection of the 100-nm and 500-nm thick InGaN films, respectively.

It can be seen from Fig. 1(a) that the 100-nm thick InGaN film is in a fully strained state as the central point with the maximum diffraction intensity of the InGaN diffraction profile is exactly located on the vertical line ($R = 0$), whereas the 500-nm thick InGaN film relaxes with a relaxation degree of about 21% calculated from the RSM.[13]

Then influences of the Si doping in InGaN on the structural and optical properties of the InGaN epilayers are investigated. Thickness values of all the samples are 500 nm and the indium compositions in InGaN films are all about 5%, determined by HRXRD measurement. The electron concentrations in the samples are measured by the Hall measurement (Table 1) on the assumption that the Si doping concentration equals the electron concentration.

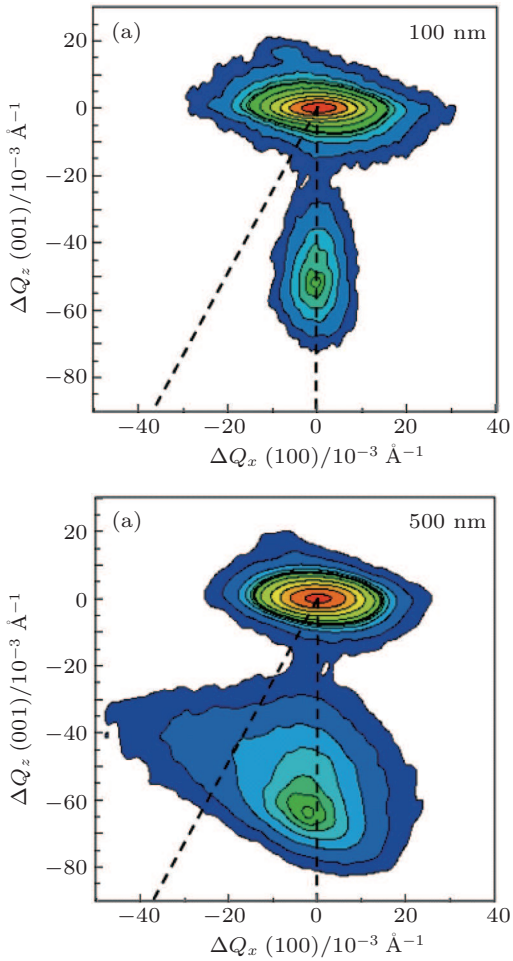


Fig. 1. (color online) Reciprocal space maps of the InGaN films with thickness values of (a) 100 nm, (b) 500 nm. The dashed lines passing through the GaN template reciprocal lattice point (RLP) correspond to the fully strained ($R = 0$) and fully relaxed ($R = 1$) states.

Table 1. Carrier concentrations and V-shaped defect densities of the InGaN films with different SiH_4 mole flow rates.

SiH_4 mole flow rate/(nmol/min)	0	0.32	1.28	2.24	3.20
Electron concentration/cm^{-3}	1.2×10^{17}	8.5×10^{17}	5.7×10^{18}	9.5×10^{18}	1.4×10^{19}
V-shaped defects density/cm^{-2}	4.3×10^{8}	2.7×10^{8}	2.4×10^{8}	2.2×10^{8}	1.9×10^{8}

Figure 2 shows the AFM three-dimensional (3D) images of the samples (3 μm×3 μm) with different Si doping concentrations of (a) 0 (undoped), (b) 5.73×10^{18} cm^{-3}, and (c) 1.43×10^{19} cm^{-3}. From the AFM data, the obtained values of root-mean-square (RMS) roughness of the samples are 38.9 nm, 32.7 nm, 20.8 nm, respectively. Apparently, the surface morphology of the InGaN is observed to be improved by Si doping. Figure 3 shows the SEM images of the same samples. These images illustrate that there exist lots of inverted pyramid V-defects on the surfaces of the InGaN films without or with Si doping. Obviously, the density of V-defects decreases after Si doping in InGaN. Table 1 also shows the V-shaped defect densities of all the samples with different Si doping concentrations. It was reported that In atom reduced Ga incorporation on the $\{1\ 0\ \bar{1}\ 1\}$ pyramid plane in comparison to that on the (0 0 0 1) surface during growth of InGaN at a medium temperature (780 °C),[14,15] which led to the formation of V-defects in InGaN. However, during the growth of InGaN with Si doping, Si atom acted as surfactant which improved the mobility of Ga along $(1\ 0\ \bar{1}\ 1)$ face, promoted the growth of InGaN in V-defect area and further suppressed the spread of V-defects. Thus, V-defects in InGaN decreased af-

ter Si doping, and meanwhile the surface morphology of the InGaN was improved due to the reduction of V-defects.

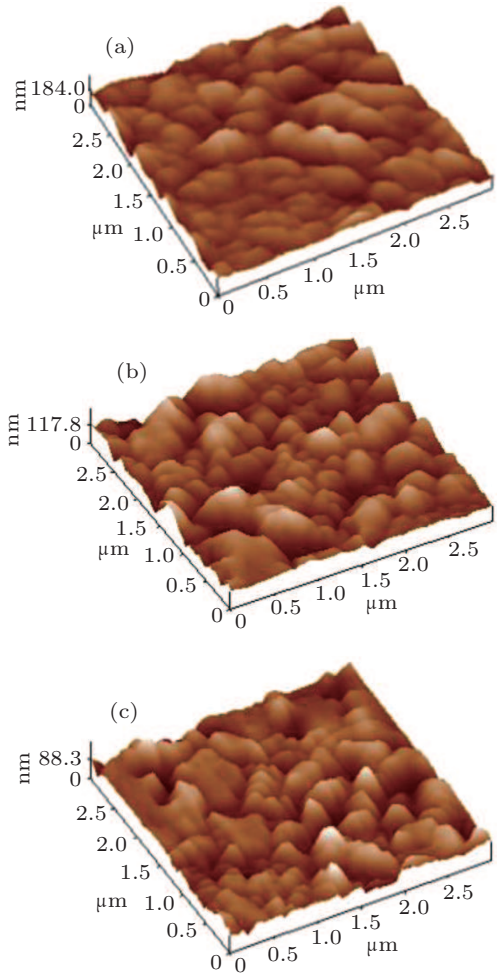


Fig. 2. (color online) AFM 3D images of InGaN films with Si doping concentrations of (a) 0 (undoped), (b) 5.73×10^{18} cm^{-3}, and (c) 1.43×10^{19} cm^{-3}.

Figure 4(a) shows (0 0 0 2) 2θ–ω scan of the InGaN/GaN with different Si doping concentrations, and figure 4(b) shows values of full width at half maximum (FWHM) of (0 0 0 2) rocking curve of the GaN and InGaN, respectively. Figure 4(a) illustrates that the influence of Si doping on indium content in the InGaN can be ignored because the 2θ values corresponding to the InGaN films are almost constant as shown in the figure. Figure 4(b) indicates that the values of FWHM of the InGaN epilayers decrease with SiH_4 mole flow rate increasing, however FWHM of the underlying GaN almost remains constant. Moreover, the tendency of FWHM is abrupt when the SiH_4 mole flow rate increases from 0 nmol/min to 0.32 nmol/min and then becomes gradual with the increase of SiH_4 mole flow rate. The results suggest that the crystal quality of the InGaN epilayer is improved by Si doping, while the improvement becomes saturated with the increase of Si doping concentration.

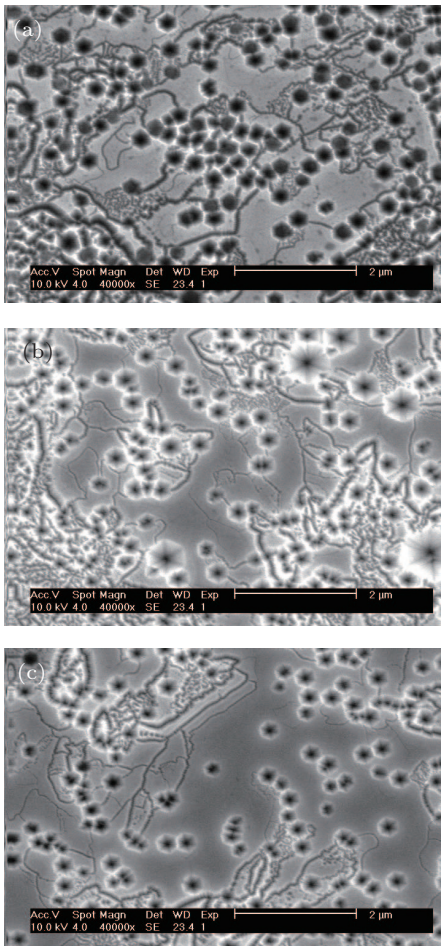


Fig. 3. SEM images of InGaN films with Si doping concentrations of (a) 0 (undoped), (b) 5.73×10^{18} cm^{-3}, and (c) 1.43×10^{19} cm^{-3}.

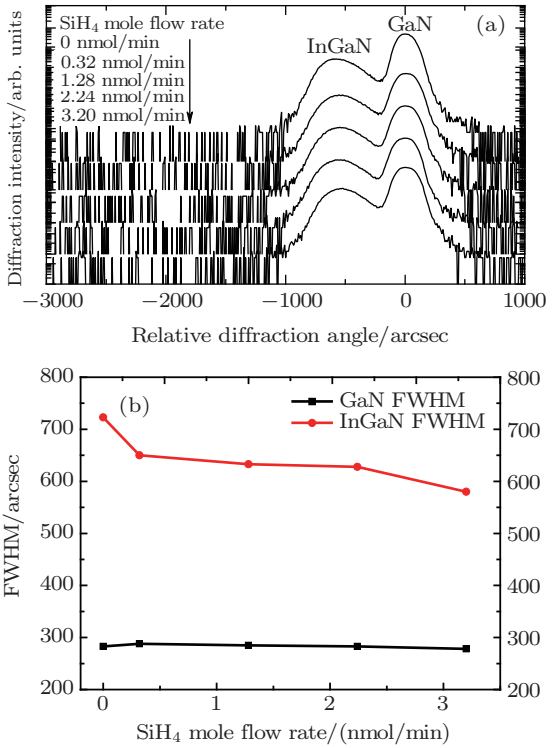


Fig. 4. (color online) (a) (0 0 0 2) 2θ–ω scan of InGaN/GaN with different SiH4 mole flow rates and (b) FWHMs of GaN and InGaN.

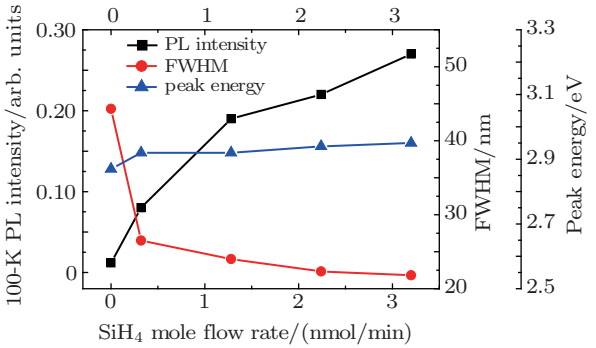


Fig. 5. (color online) Dependencies of low-temperature (100 K) PL intensity (black squares), FWHM (red circles), and peak energy (blue triangles) on SiH_4 mole flow rate.

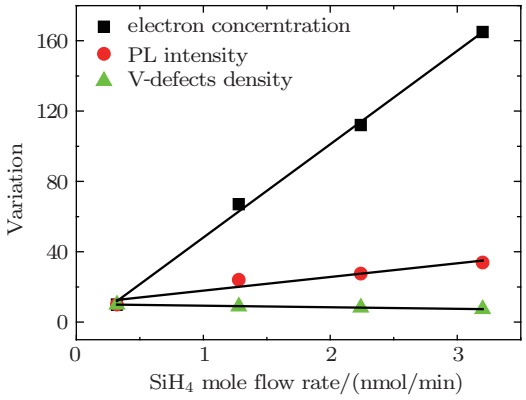


Fig. 6. (color online) Variations of electron concentration, PL intensity, and V-defects of the four Si-doped samples with SiH_4 mole flow rate.

Figure 5 displays the dependencies of low-temperature (100 K) PL intensity, FWHM, and peak energy on SiH_4 mole flow rate. It is found that the PL intensity is enhanced with SiH_4 mole flow rate increasing and the intensity of the sample with the highest Si doping concentration is over 20 times stronger than that of the undoped one. However, the emission peak almost remains constant and the FWHM value abruptly decreases first after Si doping, then slightly narrows with SiH_4 mole flow rate increasing. These findings illustrate that Si doping has little influence on indium content in the InGaN and it may improve the crystal quality of InGaN, which is in accordance with the XRD measurements. There are two possibilities that are responsible for the improvement of emission efficiency of the InGaN film with Si doping. On the one hand, the crystal quality improves and V-defects decrease in the InGaN film after the Si doping. It was reported that V-defects act as nonradiative recombination centers which would reduce the PL intensity.[16,17] Therefore, in our case the emission efficiency improves after the Si doping as it efficiently suppresses the formation of V-defects. On the other hand, Si doping leads to the increase of the electron concentration and further promotion of the overlap of electrons and holes wavefunction,[10] hence, the emission efficiency becomes increasingly high with the increase of the Si doping concentration. Figure 6 compares the variations of PL intensity, electron concentration, and V-defects of the four Si-doped samples with SiH_4 mole flow rate, and it is found that the variation rate of the electron concentration is much greater than that of V-defects with the SiH_4 mole flow rate. Based on the above analyses, it is suggested that the increase of the electron concentration plays a more important role in enhancing the PL efficiency, despite suppressing the formation of V-defects by the Si doping.

4. Conclusion

Influences of the Si doping on the structural and optical properties of the InGaN epilayers are investigated by using HRXRD, PL, AFM, and SEM. It is found that the Si doping in the InGaN can improve the surface morphology and crystal quality of the InGaN film. Meanwhile, it is observed that the Si doping, on the one hand, leads to the increase of the electron concentration and further increase in doping promotes the overlap of electron and hole wavefunction in InGaN film, on the other hand, the Si doping suppresses the formation of V-defects, which act as nonradiative recombination centers in the InGaN. The emission efficiency of the InGaN film is greatly enhanced by the Si doping and it is proposed that the former plays a more important role in enhancing the emission efficiency in the InGaN.

References

[1] Nakamura S, Senoh M, Nagahama S, Lwasa N, Yamada T, Matsushita T, Kiyoku H and Sugimoto Y 1996 *Jpn. J. Appl. Phys.* **35** L74
[2] Chichibu S, Azuhata T, Sota T and Nakamura S 1997 *Appl. Phys. Lett.* **70** 2822
[3] Mukai T, Yamada M and Nakamura S 1999 *Jpn. J. Appl. Phys.* **38** 3976
[4] Lu T P, Li S T, Zhang K, Liu C, Xiao G W, Zhou Y G, Zheng S W, Yin Y A, Wu L J, Wang H L and Yang X D 2011 *Chin. Phys. B* **20** 108504
[5] Lu T P, Li S T, Zhang K, Liu C, Xiao G W, Zhou Y G, Zheng S W, Yin Y A, Wu L J, Wang H L and Yang X D 2011 *Chin. Phys. B* **20** 098503
[6] Pei X J, Guo L W, Wang X H, Wang Y, Jia H Q, Chen H and Zhou J M 2009 *Chin. Phys. Lett.* **26** 028101
[7] Kanie H and Yoshimura T 2003 *Phys. Status Solidi (c)* **0** 2729
[8] Wang X H, Guo L W, Jia H Q, Xing Z G, Wang Y, Pei X J, Zhou J M and Chen H 2009 *Appl. Phys. Lett.* **94** 111913
[9] Kusakabe K, Hara T and Ohkawa K 2005 *J. Appl. Phys.* **97** 04503
[10] Ryu M Y, Yu Y J, Shin E J, Yu P W, Lee J I, Yu S K, Oh E S, Nam O H, Sone C S, Park Y J and Kim T I 2000 *Solid State Commun.* **116** 675
[11] Uchida K, Tang T, Goto S, Mishima T, Niwa A and Gotoh J 1999 *Appl. Phys. Lett.* **74** 1153
[12] Nakamura S 1991 *Jpn. J. Appl. Phys.* **30** L1705
[13] Pereira S, Correia M R, Pereira E, O'Donnell K P, Alves E, Sequeira A D, Franco N, Watson I M and Deatcher C J 2002 *Appl. Phys. Lett.* **80** 3913
[14] Chen Y, Takeuchi T, Amano H, Akasaki I, Yamada N, Kaneko Y and Wang S Y 1998 *Appl. Phys. Lett.* **72** 710
[15] Norhrup J E and Romano L T 1999 *Appl. Phys. Lett.* **74** 2319
[16] Li D B, Liu Y H, Katsuno T, Nakao K, Nakamura K, Aoki M, Miyake H and Hiramatsu K 2006 *Phys. Status Solidi (c)* **3** 1944
[17] Li D B, Katsuno T, Nakao K, Aoki M, Miyake H and Hiramatsu K 2006 *J. Crystal Growth* **290** 374